



PERGAMON

Available online at www.sciencedirect.com

SCIENCE @ DIRECT®

International Journal of Rock Mechanics & Mining Sciences 40 (2003) 929–937

International Journal of
Rock Mechanics
and Mining Sciences

www.elsevier.com/locate/ijrmms

Technical Note

Estimates of rock joint shear strength in part of the Fimiston open pit operation in Western Australia

D.R. Wines, P.A. Lilly*

Sinclair Knight Merz Pty Ltd, Melbourne, Australia

Western Australian School of Mines, Curtin University of Technology, PMB 22, Kalgoorlie, WA 6430, Australia

Accepted 11 February 2003

1. Introduction

1.1. Background

The city of Kalgoorlie-Boulder is situated approximately 600 km to the east of Perth in Western Australia. The Fimiston open pit (or 'super pit') is located on the eastern boundary of the city and is mining an area traditionally known as the Golden Mile. The area has been continuously worked since 1893, predominantly by underground mining methods and more recently through open cut development. Various small-scale open pits were developed in the early to mid-1980s and the amalgamation of these pits was realised in May 1989 with the formation of Kalgoorlie Consolidated Gold Mines Pty Ltd. (KCGM), a joint venture between Normandy Mining Ltd. (now Newmont Mining Corporation) and Homestake Gold of Australia Ltd.

1.2. Geology

Clout and others [1] provide a comprehensive description of the geology in this part of Western Australia and much of the information provided in this section has been sourced from this work. The Kalgoorlie goldfields are situated within the north north west striking Archaean Norseman-Wiluna Greenstone Belt. The succession consists of a 3000–4000 m thick sequence of ultramafic to mafic volcanic rocks and mafic sills, which is overlain by a 1 km thick sequence of volcano-sedimentary rocks. The gold deposits are predominantly

hosted by the ultramafic and mafic rocks. The main rock types encountered in the area are as follows:

- The Golden Mile Dolerite (GMD) is a differentiated gabbroic sill, with a thickness ranging from 600 to 940 m.
- The Paringa Basalt (PB) consists of pillowed to massive basalts with minor thin interflow sediments, approximately 850 m thick.
- The Black Flag Beds (BFB) are a sequence of sediments and felsic volcanics with a thickness of up to 1000 m. The thickness is reduced in the vicinity of the Golden Mile due to the influence of folding.
- Porphyry Dykes (PD) crosscut all formations in the stratigraphic sequence and range from 0.5 to 10 m in width in the study area.

1.3. Data collection

Geotechnical data were required in order to design a major part of the eastern wall in the Fimiston open pit and details of the data collected are discussed elsewhere [2]. However, the following provides a summary:

- Ten linear scanlines were undertaken, in which a total of 349 m of scanline were mapped for a total of 770 discontinuity measurements. Scanline mapping provided a significant amount of valuable geotechnical information and was particularly well suited to the study area where significant lengths of wall exposure are available.
- A total of 1022 m of diamond drill core were logged with 1795 discontinuity measurements taken. Most holes are oriented at relatively high angles to the dominant structures, which helped to minimise bias. Samples for laboratory shear testing were selected from these holes.

*Corresponding author. Tel.: +61-8-9088-6150; fax: +61-8-9088-6151.

E-mail address: lillyp@wasm.curtin.edu.au (P.A. Lilly).

1.4. Joint sets

Details of the rock mass domains and rock mass classification parameters are discussed elsewhere [3]. However, descriptions of the four major joint sets are summarised below:

- Joints in Set 1 are generally rough, planar and clean, with occasional quartz infill and have an average dip/dip direction of $65^\circ/271^\circ$.
- Joints in Set 2 are generally rough and planar to undulating, with regular quartz infill and have an average dip/dip direction of $2^\circ/306^\circ$.
- Joints in Set 3 are generally rough and planar, with regular quartz infill and have an average dip/dip direction of $82^\circ/323^\circ$.
- Joints in Set 4 include tightly healed, rough and undulating quartz veins and have an average dip/dip direction of $86^\circ/001^\circ$.

2. Estimating shear strength and deformation parameters

2.1. Laboratory testing

Laboratory testing generally involves a constant normal load and an increasing shear load being applied to the sample. Both shear and normal loads are monitored, as well as displacement parallel and normal to the plane of shearing. Once the peak strength is reached, displacement is continued, usually at a significantly lower shear load (reflecting the residual strength). The limit to which displacement can be measured varies between different machines. Where the limit does not allow the residual strength to be reached, the upper half specimen may be returned to its original position and the testing continued.

Multistage testing refers to the case where several tests are undertaken at different normal loads. The peak and residual shear strength can be estimated for each test from plots of the shear displacement versus shear stress. A plot of normal stress versus shear stress can then be drawn allowing estimates to be made of the shear strength characteristics of the discontinuity. The same discontinuity sample is often used for multistage testing [4] due to the difficulties in obtaining a sufficient number of identical samples, which allows the maximum information to be gained from each sample. However, Barton [5] reported that when the same sample is used, only those tests performed at low normal stress would provide reliable information on the peak strength characteristics of the discontinuity. Repeated shearing of the specimen will cause the remainder of the test results to fall somewhere between the peak and the residual values.

2.2. Barton's criterion

After recognising the inadequacy of the linear Coulomb model, Barton [5] proposed an empirical criterion for the shear strength of rock joints, as follows:

$$\tau_p = \sigma_n \tan \left[\text{JRC} \log_{10} \left(\frac{\text{JCS}}{\sigma_n} \right) + \phi_b \right], \quad (1)$$

where τ_p is the peak shear strength of the unfilled joint (that is, there is rock-to-rock contact across the plane), σ_n is the effective normal stress acting on the joint, JRC is the joint roughness coefficient (ranging from 0 to 20), JCS is the unconfined compressive strength of the rock immediately surrounding the joint and ϕ_b is the basic friction angle. The basic friction angle is a measurement of the shear strength along an artificially planar saw cut surface and is characteristic of the rock mineralogy [6].

There are some constraints on the use of the criterion, as follows:

- Barton and Choubey [7] recommended that the peak shear strength curves should be truncated for design purposes at a maximum allowable shear strength given by $\arctan(\tau/\sigma_n) = 70^\circ$.
- For unfilled joints the roughness and compressive strength of the walls are important, whereas in the case of filled joints the physical properties of the material separating the joint walls are of primary concern. Barton's criterion is only valid where joint walls are in rock-to-rock contact [7].
- Due to the relatively low normal stress levels involved in the determination of the criterion, Hoek and Bray [8] reported that the criterion is valid for the normal stress range $0.01 < \sigma_n/\text{JCS} < 0.3$.

The techniques available for estimating the input parameters to Barton's criterion are discussed below.

2.2.1. Estimation of JCS

Where the state of weathering of both the rock material and the joint walls is similar, samples of rock material tested in uniaxial compression can be used to estimate JCS. Where joint walls are weathered to a limited depth, methods of point load testing [8] and Schmidt hammer [6] techniques may be appropriate. Where no direct measurements are available, a ratio of JCS/σ_c equal to $\frac{1}{4}$ may be used [5] or field index testing may be used.

2.2.2. Estimation of JRC

Barton and Choubey [7] report that JRC could be estimated through the back analysis of shear tests, where Eq. (1) is rearranged into the following form:

$$\text{JRC} = \frac{\arctan(\tau/\sigma_n) - \phi_b}{\log_{10}(\text{JCS}/\sigma_n)}. \quad (2)$$

They also described a residual tilt test in which pairs of flat sawn surfaces are mated and the pairs of blocks are tilted until sliding occurs. If α_s is the tilt angle at which sliding starts to occur, σ_{n0} is the normal stress acting on the joint when sliding begins to occur and ϕ_r is the residual friction angle, the JRC value can be estimated from the following equation:

$$JRC = \frac{\alpha_s - \phi_r}{\log_{10}(JCS/\sigma_{n0})} \quad (3)$$

The normal stress is calculated using

$$\sigma_{n0} = \frac{W \cos \beta_s}{A}, \quad (4)$$

where W is the weight of the upper block, A is the gross contact area, and β_s is the inclination angle. Other estimation methods include the following:

- Barton and Choubey [5] profiled 136 joint surfaces prior to shear box testing, estimated JRC values from the back analysis of the shear box tests, selected the most typical profiles and published these in the form of a reference chart.
- Barton and Bandis [9] present a method for estimating JRC from the J_r component of the Q rock mass classification system.

2.2.3. Estimation of ϕ_b

The basic friction angle can be estimated from direct shear testing on smooth rock surfaces that have been prepared by means of a smooth, clean diamond saw cut [8]. Barton and Choubey [7] reported that the basic friction angle for most smooth unweathered rock surfaces lies between 25° and 35°. Table 1 shows their results, in which joints in relatively fresh rock were most frequently prepared by diamond saw.

Stimpson [10] suggested the use of tilt testing of diamond core samples for the estimation of the basic friction angle. He observed that the core surfaces produced by typical core drilling procedures are pre-cut and smooth and therefore not dissimilar to a saw cut rock surface. The suggested tilt tests involve attaching two pieces of core to a horizontal base, ensuring that the core samples are in contact with one another and are not free to slide. A third piece of core is then placed on top of the first two pieces and the base is rotated about a horizontal axis until sliding of the upper piece of core along the two line contacts with the lower pieces of core begins. The following equation can then be used to estimate the basic friction angle.

$$\phi_A = \tan^{-1}(1.155 \tan \alpha_s), \quad (5)$$

where ϕ_A is the basic friction angle for the upper piece of core and α_s is the angle at which sliding commences.

Table 1
Basic friction angles for various unweathered rocks obtained from flat and residual surfaces [7]

Rock type	Moisture condition	Basic friction angle ϕ_b
Sandstone	Dry	26–35
Sandstone	Wet	25–33
Sandstone	Wet	29
Sandstone	Dry	31–33
Sandstone	Dry	32–34
Sandstone	Wet	31–34
Sandstone	Wet	33
Shale	Wet	27
Siltstone	Wet	31
Siltstone	Dry	31–33
Siltstone	Wet	27–31
Conglomerate	Dry	35
Chalk	Wet	30
Limestone	Dry	31–37
Limestone	Wet	27–35
Basalt	Dry	35–38
Basalt	Wet	31–36
Fine-grained granite	Dry	31–35
Fine-grained granite	Wet	29–31
Coarse-grained granite	Dry	31–35
Coarse-grained granite	Wet	31–33
Porphyry	Dry	31
Porphyry	Wet	31
Dolerite	Dry	36
Dolerite	Wet	32
Amphibolite	Dry	32
Gneiss	Dry	26–29
Gneiss	Wet	23–26
Slate	Dry	25–30
Slate	Dry	30
Slate	Wet	21

2.2.4. Scale effects

Barton and Choubey [7] noted significant scale effects in relation to JRC and JCS. As the joint length increases, joint wall contact is transferred to the larger and less steeply inclined asperities as the peak shear strength is approached, resulting in larger individual contact areas with correspondingly lower JCS values. The larger contact areas will also be less steeply inclined in relation to the mean plane of the joint when compared to the small, steep asperities, resulting in reduced JRC values. Consequently, the reduction in JRC and JCS values will result in a reduction in shear strength as the discontinuity length is increased.

Barton and Bandis [11] proposed the following correction factors after undertaking extensive joint and joint replica testing and a literature review:

$$JRC_n \approx JRC_0 \left[\frac{L_n}{L_0} \right]^{-0.02JRC_0}, \quad (6)$$

$$JCS_n \approx JCS_0 \left[\frac{L_n}{L_0} \right]^{-0.02JRC_0}, \quad (7)$$

where the subscripts “0” and “n” refer to laboratory scale (100 mm) and in situ block sizes, respectively. The JRC and JCS values used in Eq. (1) refer to laboratory scale parameters (that is, JRC_0 and JCS_0).

3. Discontinuity stiffness characteristics

Joint stiffness parameters describe the stress-deformation characteristics of the joint and are fundamental properties in the numerical modelling of jointed rock. Joint shear stiffness and joint normal stiffness are discussed below.

3.1. Joint shear stiffness

Barton [12] described joint shear stiffness (K_s) as the average gradient of the shear stress-shear displacement curve for the section of the curve below peak strength. Shear stiffness can be estimated from direct shear testing results, and its value will depend on the size of a sample tested and will generally increase with an increase in normal stress [13]. Barton and Choubey [7] suggested the following equation for the estimation of the peak shear stiffness (MPa/m):

$$K_s = \frac{100}{L_x} \sigma_n \tan [JRC \log_{10}(JCS/\sigma_n) + \phi r], \quad (8)$$

where L_x is the joint length in metres. Use of the equation requires the assumption that the peak shear strength is reached after the shearing of approximately 1% of the joint length. If the scale effect does not die out within the critical discontinuity length (L_{crit}), the value of L_x should not exceed L_{crit} .

The UDEC user’s manual [14] states that the shear stiffness for rock joints with clay-infilling can range from roughly 10–100 MPa/m while that for tight joints in granite and basalt can exceed 100 GPa/m. Coulthard [15] presents typical ranges for joint shear stiffness including values of 250–450 GPa/m for jointing in basalt.

3.2. Joint normal stiffness

Barton [12] describes joint normal stiffness (K_n) as the normal stress per unit closure of the joint. Bandis et al. [13] proposed that joint normal stiffness is influenced by

- the initial actual contact area;
- the joint wall roughness;
- the strength and deformability of the asperities; and
- the thickness, type and physical properties of any infill material.

Joint normal stiffness can be estimated from laboratory testing. The UDEC user’s manual [14] states that

the normal stiffness for rock joints with clay-infilling can range from roughly 10 to 100 MPa/m while that for tight joints in granite and basalt can exceed 100 GPa/m. Coulthard [15] presents typical ranges for joint normal stiffness including values of 300–550 GPa/m for basalt.

4. Direct shear testing for the study area

A number of multistage direct shear tests (DSTs) have been undertaken on samples of Joint Set 1 from both PB and GMD. Joint Set 1 was chosen for detailed study as it dips to the west and was therefore deemed to be the most critical to the stability of the eastern wall batters. The testing was performed by Western Geotechnics Pty Ltd in Perth and the Western Australian School of Mines in Kalgoorlie prior to the commencement of the present study and the results are summarised in Table 2. The frequency histograms from which the distribution types shown in Table 2 have been identified are presented in Figs. 1 and 2.

5. Application of Barton’s criterion to the study area

5.1. JCS and JRC

A summary of the JCS and JRC estimates for the four main joint sets are presented in Table 3. The discontinuities in the study area generally exhibit no wall softening due to weathering, and the JCS is therefore assumed to be equal to the UCS of the intact rock. JRC values for the four discontinuity sets in the study area were recorded during scanline mapping and diamond core logging using the profiles of Barton and Choubey [7].

Table 2
Summary of direct shear test results for Joint Set 1

Parameter	Statistic	PB 17 tests	GMD 35 tests
Peak cohesion (kPa)	Mean	352.5	134.7
	SD	99.9	124.5
	CoV (%)	28.3	92.4
	Min	100	10
	Max	650	462.1
	Distribution type	Normal	Log normal
Peak friction angle (deg)	Mean	34.9	40.5
	SD	5.5	6.7
	CoV (%)	15.8	16.5
	Min	22	20
	Max	51	60
	Distribution type	Log normal	Log normal

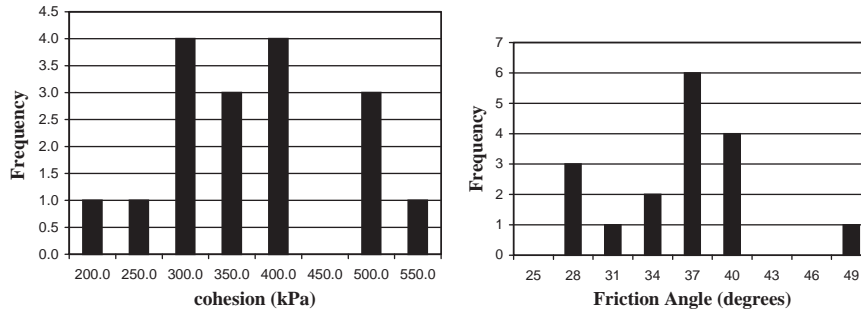


Fig. 1. Cohesion and friction histograms for PB Joint Set 1.

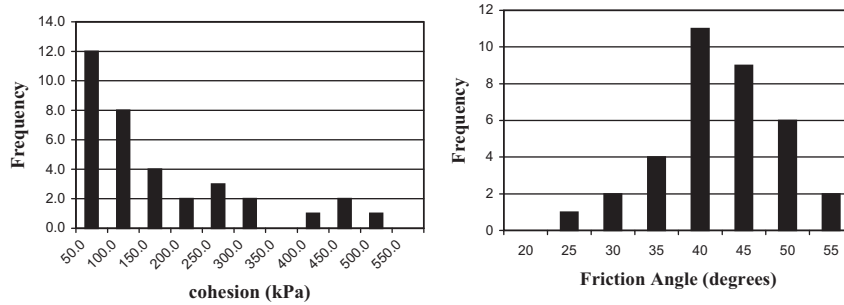


Fig. 2. Cohesion and friction histograms for GMD Joint Set 1.

Table 3
JCS and JRC estimates for the four main joint sets

Parameter	Statistic	PB			GMD			
		Set 1	Set 2	Set 4	Set 1	Set 2	Set 3	Set 4
JCS (MPa)	Mean	86.9	86.9	86.9	95.9	95.9	95.9	95.9
	SD	28.9	28.9	28.9	34.4	34.4	34.4	34.4
	Min	43.7	43.7	43.7	34.3	34.3	34.3	34.3
	Max	156.5	156.5	156.5	156.3	156.3	156.3	156.3
JRC	Mean	6.4	7.1	4.7	7.8	7.3	5.9	7.0
	SD	3.0	2.8	2.9	2.7	2.3	2.2	3.1
	Min	2.0	2.0	2.0	2.0	2.0	2.0	2.0
	Max	14.0	12.0	10.0	16.0	14.0	10.0	14.0

5.2. Basic friction angle

The basic friction angle has been estimated using three different methods, as follows:

- Direct shear testing (undertaken prior to the commencement of this study) was performed along saw cut samples of both PB and GMD and the results are summarised in Table 4. The frequency histograms for the test results are presented in Fig. 3 and the probability distribution types were estimated from these histograms.
- A total of 88 tilt tests were undertaken on split core in both the basalt (42 tests) and the dolerite (46 tests). The basic friction angle was then calculated using Eq. (5).

Table 4
Summary of direct shear testing results on saw cut surfaces

Parameter	Statistic	PB	GMD
		10 tests	5 tests
Basic Friction Angle (deg)	Mean	36.9	34.2
	SD	2	1.5
	Min	32.9	32
	Max	39.4	36
Distribution type		Uniform	Uniform

- Table 1 provides suggested values for the basic friction angles for both dry basalt and dry dolerite.

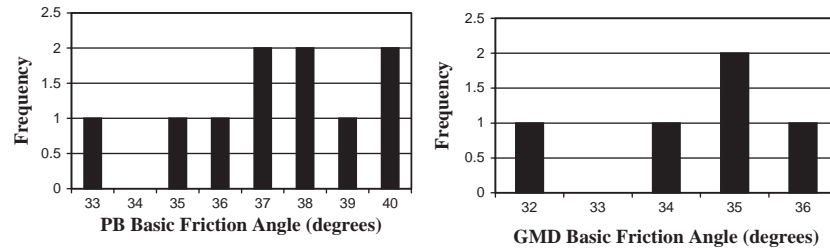


Fig. 3. Basic friction angle histograms for PB and GMD.

Table 5
Basic friction angle estimates

Rock	Direct shear testing				Tilt testing				Values from Table 1
	Mean	SD	Min	Max	Mean	SD	Min	Max	
PB	36.9	2	32.9	39.4	39.6	1.1	37.4	42.1	35–38
GMD	34.2	1.5	32	36	36.3	1.4	32.6	40	36

Table 6
Shear stiffness values for GMD

Stage no.	Approx. normal stress (kPa)	K_s (MPa/m)
1	200	46.1
2	500	74.8
3	900	116.9

Table 7
Peak shear stiffness estimates using Eq. (8)

Normal stress (kPa)	PB K_s (MPa/m)	GMD K_s (MPa/m)
200	4.7	4.6
500	10.7	10.3
900	18.1	17.4

The basic friction angles estimated by each of these three methods are presented in Table 5.

6. Joint shear and normal stiffness estimates

The three-stage direct shear testing results for GMD include shear stress and shear displacement data at the peak shear strength. The normal stress values applied during stages 1, 2 and 3 were approximately 200, 500 and 900 kPa for each test. The shear stress and shear displacement data from each test were combined for each stage, allowing shear stiffness values to be estimated for each value of normal stress. The resulting values are presented in Table 6. The results provided by Eq. (8) are presented in Table 7, with the average trace length for Joint Set 1 being applied. No laboratory test results are available for the estimation of joint normal stiffness.

7. Discussion and conclusions

7.1. Basic friction angle estimates

From the basic friction angle estimates presented in Table 5, the following observations can be

made:

- The estimates produced by direct shear testing are lower than those produced by tilt testing for both rock types. This could be the result of one or both of the following factors:
 - (1) the direct shear testing was undertaken using a four stage testing procedure on each of the basalt samples and a 3 stage testing procedure on each of the dolerite samples. Any small-scale surface irregularities may have been sheared off by the initial stages of the tests, resulting in flatter curve and a lower basic friction angle. There is significantly less potential for the shearing of asperities during tilt testing due to the relatively low normal stress levels involved; and/or
 - (2) the outside surface of the core used for tilt testing may have been relatively uneven when compared to the saw cut surfaces. As a part of the tilt testing procedure, each core sample was inspected for visual irregularities caused by the drilling process. Only those samples that appeared to be smooth were used for testing. However, this process may not have identified small irregularities and these may have influenced the tilt testing results.

- The value obtained for the basalt from direct shear testing is within the range recommended in Table 1. The value obtained by tilt testing is above this range.
- The value obtained for the dolerite by tilt testing is very close to that recommended in Table 1.
- Standard deviations are higher for the DST data when compared to the tilt testing data. This may be explained by the significantly greater number of tilt tests undertaken for each rock type.

Interestingly, the peak friction angle estimated from direct shear testing along Joint Set 1 in PB is lower than the basic friction angle estimated from direct shear testing along saw cut surfaces. This may be explained by an increase in the shearing of surface asperities caused by the relatively high normal stress levels (from 400 to 3500 kPa) used in the testing of the natural surfaces. Subsequent flattening of the failure envelope may have led to the relatively low friction angle and the relatively high cohesion value.

The DST data are considered more reliable than the tilt testing data and are therefore used in the implementation of Barton’s criterion. Also, the JCS values are probably being over-estimated by assuming the joint walls to be completely unaffected by weathering. Using the more conservative basic friction angle estimates may reduce or eliminate any subsequent over-estimation in shear strength. Table 8 summarises Barton’s criterion input parameters for the four main joint sets in the study area.

7.2. Comparison between estimates

As noted above, Barton’s criterion is only strictly valid for the normal stress range $0.01 < \sigma_n / JCS < 0.3$

and, on this basis, its use becomes invalid in PB and GMD at normal stress levels of less than approximately 8.5 MPa. Notwithstanding this apparent conflict we present Figs. 4 and 5, which show normal stress versus

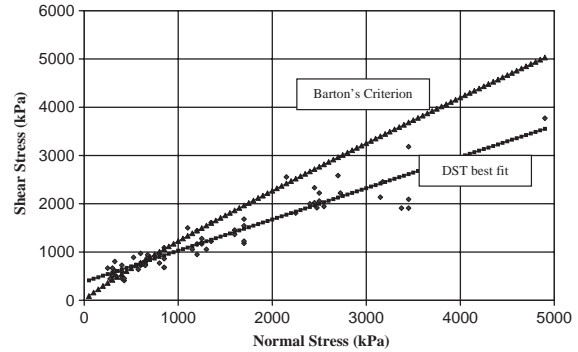


Fig. 4. Comparison between DST results and Barton’s criterion results for PB.

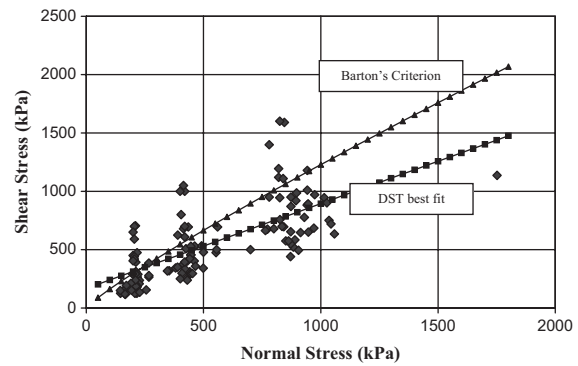


Fig. 5. Comparison between DST and Barton’s criterion results for GMD.

Table 8
Barton’s criterion input parameters

Parameter	Statistic	PB			GMD			
		Set 1	Set 2	Set 4	Set 1	Set 2	Set 3	Set 4
JCS (MPa)	Mean	86.9	86.9	86.9	95.9	95.9	95.9	95.9
	SD	28.9	28.9	28.9	34.4	34.4	34.4	34.4
	Min	43.7	43.7	43.7	34.3	34.3	34.3	34.3
	Max	156.5	156.5	156.5	156.3	156.3	156.3	156.3
JRC	Mean	6.4	7.1	4.7	7.8	7.3	5.9	7.0
	SD	3.0	2.8	2.9	2.7	2.3	2.2	3.1
	Min	2.0	2.0	2.0	2.0	2.0	2.0	2.0
	Max	14.0	12.0	10.0	16.0	14.0	10.0	14.0
Basic friction angle (deg)	Mean	36.9	36.9	36.9	34.2	34.2	34.2	34.2
	SD	2.0	2.0	2.0	1.5	1.5	1.5	1.5
	Min	32.9	32.9	32.9	32.0	32.0	32.0	32.0
	Max	39.4	39.4	39.4	36.0	36.0	36.0	36.0

shear stress plots for:

- the DST data for natural discontinuities;
- the corresponding least squares best-fit lines for the DST data; and
- the results produced by Barton's criterion, in PB and GMD, respectively.

The envelopes produced by each method intersect at a normal stress level of approximately 700 kPa for PB and approximately 300 kPa for GMD. Below these normal stress levels, Barton's criterion produces a lower shear strength envelope, while above these levels the direct shear testing provides a lower shear strength envelope.

Because the direct shear testing was undertaken using three and four stage testing procedures, surface asperities were probably sheared off during the initial stages of the tests. This would result in a flatter curve and a lower friction angle when compared to the Barton's criterion results, since the latter provides an estimate of peak shear strength. In support of this explanation, the Barton's criterion results correlate relatively well with the first stage direct shear testing results in which the asperities are relatively intact.

7.3. Variability

The coefficients of variation (CoV) for the direct shear testing results along Joint Set 1 are presented in Table 2. The values of 15.8 and 16.5% for the friction angle in PB and GMD, respectively, correspond well with the range proposed by Lilly [16] of 10–15%. The values of 28.3% and 92.4% for the cohesion of PB and GMD, respectively, are significantly different from the value of 40% proposed by Lilly [16]. Notwithstanding this, the test results do confirm that the variability is greater for cohesion than for friction angle.

The distribution shapes for GMD are more clearly defined (Fig. 2 from 35 tests) than those for PD (Fig. 1 from only 17 tests), although neither is particularly definitive. The lognormal (tending to exponential) shape of the GMD cohesion distribution is due to the fact that the mean value and standard deviation are in the same order of magnitude (CoV is almost unity), but where negative values of cohesion are not possible, thereby causing a truncation of the distribution at zero.

The choice of distribution shape in rock slope stability analysis can have a significant influence on the estimated probability of failure and, in cases where test data are insufficient to define these distributions satisfactorily (such as those for PB), the sensitivity of the failure mechanism(s) to distribution shape should be considered explicitly. However, a more detailed discussion of this point is beyond the scope of this paper.

7.4. Joint shear stiffness

The joint shear stiffness results provided by direct shear testing are significantly higher than those produced by Eq. (8). This discrepancy could possibly be explained by the influence of scale effects. The mean trace length estimates for Joint Set 1 were used in Eq. (8), whereas the direct shear testing was undertaken along samples that were significantly smaller than the mean trace length. Both methods indicate that the shear stiffness values increase with an increase in the normal stress.

Acknowledgements

This paper is based on part of a research thesis [17] submitted to the Western Australian School of Mines, Curtin University of Technology. The authors wish to acknowledge the support of KCGM (who employed the first author during the period that this work was undertaken) and for that company's permission to publish this paper.

References

- [1] Clout JMF, Cleghorn JH, Eaton PC. Geology of the Kalgoorlie Gold Field. In: Hughes FE, editor. Geology of the mineral deposits of Australia and Papua New Guinea. Melbourne: The Australasian Institute of Mining and Metallurgy, 1990. p. 411–31.
- [2] Wines DR, Lilly PA. Measurement and analysis of rock mass discontinuity spacing and frequency in part of the Fimiston Open Pit operation in Kalgoorlie, Western Australia: a case history. *Int J Rock Mech Min Sci* 2002;39(5):589–602.
- [3] Wines DW, Lilly PA. A comparative analysis of rock mass classification schemes in part of the Fimiston Open Pit operation in Kalgoorlie, Western Australia. *Aust Geomech* 2001;36(4): 59–72.
- [4] Hencher SR, Richards LR. Laboratory direct shear testing of rock discontinuities. *Ground Eng* 1989;22:24–31.
- [5] Barton N. Review of a new shear strength criterion for rock joints. *Eng Geol* 1973;7:287–332.
- [6] Giani GP. Rock slope stability analysis. Rotterdam: A.A Balkema Publishers, 1992.
- [7] Barton N, Choubey V. The shear strength of rock joints in theory and practice. *Rock Mech* 1977;10:1–54.
- [8] Hoek E, Bray JW. Rock slope engineering, 3rd ed. London: Institute of Mining and Metallurgy, 1981.
- [9] Barton N, Bandis S. Review of predictive capabilities of JRC-JCS model in engineering practice. In: Barton N, Stephansson O, editors. Proceedings of the International Symposium on Rock Joints, Loen, Norway. Rotterdam: Balkema, 1990. p. 603–10.
- [10] Stimpson B. A suggested technique for determining the basic friction angle of rock surfaces using core. *Int J Rock Mech Min Sci Geomech Abstr* 1981;18:63–5.
- [11] Barton N, Bandis S. Effects of block size on the shear behaviour of jointed rock. 23rd US Symposium on Rock Mechanics, Berkeley, CA, 1982. p. 739–60.
- [12] Barton N. A model study of rock-joint deformation. *Int J Rock Mech Min Sci Geomech Abstr* 1972;9:579–602.

- [13] Bandis SC, Lumsden AC, Barton NR. Fundamentals of rock joint deformation. *Int J Rock Mech Min Sci Geomech Abstr* 1983;20(6):249–68.
- [14] Itasca Consulting Group Inc. Universal distinct element code (UDEC), Version 3.0. Minneapolis, MN, 1996.
- [15] Coulthard, M. UDEC training course (course notes). Short Course No. 9901, Perth, 1999.
- [16] Lilly PA. Probability and risk in Geomechanics. MEngSc course notes, Mining Engineering Program, Western Australian School of Mines, Kalgoorlie, 1999.
- [17] Wines DR. Aspects of rock slope engineering at the Fimiston Open Pits. Unpublished MEng thesis, Mining Engineering Department, Western Australian School of Mines, Curtin University of Technology, 2000. 333pp.